

**Cellular internalisation of dissolved cobalt ions from
ingested CoFe₂O₄ nanoparticles: in vivo experimental
evidence**

Journal:	<i>Environmental Science & Technology</i>
Manuscript ID:	es-2012-05132g
Manuscript Type:	Article
Date Submitted by the Author:	24-Dec-2012
Complete List of Authors:	Drobne, Damjana; University of Ljubljana, Biotechnical Faculty, Department of Biology Novak, Sara; University of Ljubljana, Biotechnical Faculty, Department of Biology Golobic, Miha; University of Ljubljana, Biotechnical Faculty, Department of Biology Zupanc, Jernej; University of Ljubljana, Biotechnical Faculty, Department of Biology GIANONCELLI, ALESSANDRA; Sincrotrone Trieste S.C.p.A., ELETTRA, Kiskinova, Maya; Sincrotrone Trieste, Experimental Division Kaulich, Burkhard; Sincrotrone Trieste, Experimental Division Pelicon, Primoz; Institute Jozef Stefan, Vavpetic, Primoz; Institute Jozef Stefan, Jeromel, Luka; Institute Jozef Stefan, Ogrinc, Nina; Institute Jozef Stefan, Makovec, Darko; Institute Jozef Stefan,

SCHOLARONE™
Manuscripts

1
2
3 **Cellular internalisation of dissolved cobalt ions from ingested CoFe₂O₄ nanoparticles: *in***
4 ***vivo* experimental evidence**
5
6
7
8

9 Sara Novak[†], Damjana Drobne^{†‡§*}, Miha Golobic[†], Jernej Zupanc[†], Alessandra Gianoncelli[¶],
10 Maya Kiskinova[¶], Burkhard Kaulich[¶], Primož Pelicon[□], Primož Vaupetič[□], Luka Jeromel[□],
11 Nina Ogrinc[□], Darko Makovec[□]
12
13
14
15
16
17

18 [†]Department of Biology, Biotechnical Faculty, University of Ljubljana, Večna pot 111, 1000
19 Ljubljana, Slovenia
20

21 [‡]Centre of Excellence, Advanced Materials and Technologies for the Future (CO
22 NAMASTE), Jamova cesta 39, 1000 Ljubljana, Slovenia
23
24

25 [§]Center of Excellence, Nanoscience and Nanotechnology (Nanocentre), Jamova cesta 39, 1000
26 Ljubljana, Slovenia
27
28

29 [¶] Sincrotrone Trieste S.C.p.A. Strada Statale 14 - km 163,5 in AREA Science Park,
30
31
32 34149 Basovizza, Trieste, Italy
33
34

35 [□] Jožef Stefan Institute, Jamova cesta 39, 1000 Ljubljana, Slovenia
36

37 Corresponding author: damjana.drobne@bf.uni-lj.si
38
39
40
41
42
43
44
45
46
47
48
49
50
51
52
53
54
55
56
57
58
59
60

Abstract

1
2
3
4
5
6
7
8
9
10
11
12
13
14
15
16
17
18
19
20
21
22
23
24
25
26
27
28
29
30
31
32
33
34
35
36
37
38
39
40
41
42
43
44
45
46
47
48
49
50
51
52
53
54
55
56
57
58
59
60

With a model invertebrate animal we have assessed the fate of magnetic nanoparticles in biologically relevant media, i.e. digestive juices. The toxic potential and the internalisation of such nanoparticles by non-target cells was also examined. The aim of this study was to provide experimental evidence on the formation of Co^{2+} , Fe^{2+} and Fe^{3+} ions from CoFe_2O_4 nanoparticles in the digestive juices of a model organism. Standard toxicological parameters were observed. Cell membrane stability was tested with a modified method for assessment of cell membrane stability. Proton induced x-ray emission and low energy synchrotron radiation X-ray fluorescence was used to study internalisation and distribution of Co and Fe. Co^{2+} ions were found to be more toxic than nanoparticles. We confirmed that Co^{2+} ions are accumulated in the hepatopancreas but Fe^{n+} ions or CoFe_2O_4 nanoparticles are not retained *in vivo*. A model biological system with a terrestrial isopod is suited to studies of the potential dissolution of ions and other products from metal-containing nanoparticles in biologically complex media.

Introduction

In the past decade, magnetic nanoparticles (NPs) have attracted much attention because of their potential use in different fields such as medicine, electronics and energetic.¹

CoFe₂O₄ NPs are magnetic NPs with potential application in cell separation and purification, as contrast agents for magnetic resonance imaging (MRI), for drug delivery, as biosensors for biological targets and for magnetic fluid hyperthermia (MFH).²⁻⁸ The key issue which must be resolved before CoFe₂O₄ nanoparticles can be widely applied for medical purposes refers to dissolution of cobalt (Co) from CoFe₂O₄ nanoparticles in biological fluids. Cobalt ions (Co²⁺) may induce the formation of Reactive Oxygen Species (ROS),⁹ oxidize proteins¹⁰ and cause oxidative DNA damage¹¹ and consequently, the possible dissolution of the cobalt ions from the CoFe₂O₄ particles must be controlled.

It is now widely recognized that such dissolution plays an important role in nanoparticle toxicity, but the extent of this phenomenon remains unclear. It has been found to be influenced mainly by pH but also by the specific surface area of the nanoparticles. Natural organic compounds in the cellular media may either enhance or reduce the release of ions from nanoparticles, depending on their chemical composition and concentration.^{12, 13}

Methods used for studying dissolution include different chemical analytical methods, such as atomic absorption spectroscopy (AAS),¹⁴ inductively coupled plasma mass spectrometry (ICP-MS)¹⁵ and localized surface plasmon resonance (LSPR).¹⁶ These methods may be used in conjunction with ultracentrifugation of a suspension which separates the insoluble nanoparticles from ions that remain in solution.

Measurements of dissolved ions from particles in biological studies are useful only if they are conducted in biologically relevant media. As a rule, it is not possible to mimic biological media, therefore it is necessarily to conduct experiments in *in vivo* systems. Data on dissolution are very important in order to get an insight into potentially compromised efficiency of applied nanomaterials or their toxicity when coming in contact with biological fluids.

In the work presented here we have selected a model biological system, in which CoFe₂O₄ nanoparticles are introduced into a complex biological medium comprised of a digestive gut and digestive glands of a model terrestrial isopod crustacean. Measurements of pH in the gut of terrestrial isopods (*Porcellio scaber*) with a LIX-type pH microelectrode

1
2
3 showed pH 5.5–6.0 in the anterior hindgut, and pH 6.0–6.5 in the posterior hindgut.¹⁷ The pH
4 value of the *P. scaber* digestive glands (hepatopancreas) is 6.1 ± 0.3 and at its distal region it
5 is slightly more acidic, with pH 5.8 - 6.1.¹⁸ This biological system represents a complex
6 biological environment which acts as an assembly of biologically relevant conditions which
7 may affect dissolution of cobalt or iron ions from nanoparticulate CoFe_2O_4 .
8
9

10
11
12 Animals were fed with CoFe_2O_4 nanoparticles added on leaves in a dry, biologically
13 unreactive form. Consumed particles entered the gut and digestive system, and are retained in
14 the digestive system for 2-4 hours. Reflux of partly digested food also reaches the digestive
15 glands, but with some delay. Apart from digestion and absorption of food, one of major roles
16 of the digestive system is to accumulate metals in proportion to that in the gland lumen. In
17 bioaccumulation studies with isopods, it is expected that accumulation of a metal is related to
18 the bioavailable metal ion fraction of the gland fluid.^{19, 20}
19
20
21
22
23

24 The aim of this study was to provide experimental evidence on the formation of Co^{2+}
25 and/or $\text{Fe}^{2+}/\text{Fe}^{3+}$ ions from CoFe_2O_4 nanoparticles in the digestive juices of a model organism,
26 accumulation of dissolved ions by digestive gland epithelium, cellular internalisation of
27 particles as well as their toxic potential.
28
29
30

31 We hypothesize that metal ions are generated from ingested CoFe_2O_4 nanoparticles in
32 digestive system and that ions are accumulated by digestive gland cells proportional to
33 exposure doses. We also hypothesise that if particles enter cells they may reach a location
34 distinct from that occupied by ions that have been accumulated following other pathways.
35
36
37
38
39
40

41 **Materials and methods**

42 **Chemicals**

43
44
45
46 Acridine orange (AO), ethidium bromide (EB), sodium chloride (NaCl), potassium chloride
47 (KCl), magnesium chloride (MgCl_2), glucose and 2-amino-2-hydroxymethyl-propane-1,3-diol
48 (TRIS), were purchased from Merck. Cobalt (II) chloride hexahydrate ($\text{CoCl}_2 \cdot 6\text{H}_2\text{O}$), 99.9%
49 (metal basis) was purchased from Alfa Aesar Johnson Matthey Company. CoFe_2O_4
50 nanoparticles were synthesized at the Department for Materials Synthesis, Jožef Stefan
51 Institute in Ljubljana.
52
53
54
55
56
57
58
59
60

Model organisms

Terrestrial isopods *Porcellio scaber* (Isopoda, Crustacea) were collected in July, 2011 at an uncontaminated location near Ljubljana, Slovenia. The animals were kept in a terrarium filled with a layer of moistened soil and a thick layer of partly decomposed hazelnut tree leaves (*Corylus avellana*), at a temperature of $20 \pm 2^\circ\text{C}$ and a 16:8 h light:dark photoperiod. Only adult animals of both sexes and weighing more than 30 mg were used. If moulting or the presence of marsupia were observed, the animals were excluded from the experiment in order to keep the investigated population as physiologically homogenous as possible.

The digestive system of the terrestrial isopod *Porcellio scaber* is composed of a stomach, four blind-ending digestive gland tubes (hepatopancreas) and a gut. Food enters the digestive glands directly *via* a short stomach or after the reflux from the gut and ingested material is mixed with digestive fluids.

Characterization of nanoparticles

The nanoparticles were synthesized by co-precipitation using NaOH from aqueous solutions of Co(II) and Fe (III) ions at elevated temperatures.²⁴ The nanoparticle samples were thoroughly washed with water after the synthesis and then suspended in aqueous glucose solution. The suspended CoFe_2O_4 nanoparticles show strong agglomeration in dH_2O .

Nanoparticles were inspected with transmission electron microscopy (TEM) coupled with energy dispersive X-ray spectroscopy (EDXS) (JEOL 2010F) and Zeta potential was also measured (Brookhaven Instruments Corp., ZetaPALS). The aim of these analyses was to provide data on the suspension of particles and allow comparisons among different studies and within our experiments.

After exposure in feeding experiments, remnants of selected leaves were dried and attached to mounts with silver paint (SPI), gold-palladium sputtered (Sputter coater SCD 050, BAL-TEC) and investigated by field emission scanning electron microscopy (SEM) (Jeol JSM-6500F) at the Institute of Metals and Technology in Ljubljana. Energy dispersive X-ray analysis (EDX) was used to establish their chemical composition (EDS/WDS Oxford Instruments INCA, Jeol JSM-6500F) at the Institute of Metals and Technology.

Food preparation

Hazelnut leaves were collected in an uncontaminated area and dried at room temperature and the animals consumed particles in a suspension applied to a leaf surface.. Dried leaves were cut into pieces of approximately 100 mg. The reference material, CoCl_2 or CoFe_2O_4 nanoparticles, was suspended in distilled water before each experiment to obtain final concentrations of cobalt of 1000, 2000 and 5000 $\mu\text{g}/\text{ml}$. To diminish agglomeration, a suspension of nanoparticles in H_2O was sonicated in an ultrasonic bath for 1 h before being applied to the leaves.

In the control group, the leaves were treated with distilled water and in the test group, a suspension of particles was brushed onto the abaxial surface of leaves to give final nominal concentrations of 1000, 2000 and 5000 μg CoCl_2 or CoFe_2O_4 nanoparticles per gram (dry weight) of leaf. The leaves were allowed to stand until dry.

Experimental Procedure

Each individual animal was placed in a 9 cm Petri dish. One hazelnut leaf was treated with distilled water, or a suspension of CoCl_2 or nano- CoFe_2O_4 and placed in the dish as the animal's only food source. Humidity in the Petri dish was maintained by spraying tap water on the internal side of the lid every day. All Petri dishes were kept in a large glass container under controlled conditions in terms of air humidity ($\geq 80\%$), temperature ($21 \pm 1^\circ\text{C}$) and light regime (16:8 h light:dark photoperiod).

Different numbers of animals in each individual experiment were exposed to varying concentrations of nanoparticles for 14 days (Table S1, Supporting Information). Four experiments, A, B, C and D were performed one at the time and the exposure concentrations of suspensions and initial number of tested animals were selected on the basis of the type of analyses conducted after exposure.

The concentrations were chosen on the basis of our preliminary experiments. After exposure, the animals were anaesthetized at low temperature and then decapitated and their digestive glands isolated. In experiments, digestive gland tubes were used for different analyses (Table S1, Supporting Information).

Feeding parameters, weight change and survival

After 14 d of exposure of the animals to treated leaves, faecal pellets and leaves were removed from the Petri dishes, dried at room temperature for 24 h and weighed. The feeding rate of isopods was calculated as the mass of consumed leaves per wet weight of the animal per day. The food assimilation efficiency was calculated as the difference between the mass of consumed leaves and mass of faecal pellets divided by the mass of consumed leaf. The weight change of an animal was determined as the difference in its mass from the beginning to the end of the experiment

AO/EB Analysis: Digestive gland cell membrane stability

Cell membrane stability was tested with a modified method for assessment of cell membrane stability, previously described by Valant et al.^{21, 25}

A single isolated hepatopancreatic tube was incubated for 5 min in a mixture of the fluorescent dyes acridine orange and ethidium bromide and then put on a microscope slide. Fresh samples were photographed and examined with an Axioimager Z1 fluorescent microscope (Zeiss) with two different sets of filters. The excitation filter 450 to 490 nm and the emission filter 515 nm (filter set 09) were used to visualize AO and EB stained nuclei, while the excitation filter 365 nm and the emission filter 397 nm (filter set 01) were used to visualize nuclei stained with EB only. Cell membrane integrity was assessed by examination of micrographs. Photographs of intact digestive glands were examined by the same observer twice at intervals of at least 24 h and cell membrane integrity was rated on the scale from 0 to 9 by visual inspection. On the basis of preliminary experiments, it was concluded that non-treated (control) animals showed < 5% of nuclei stained by EB, while severely stressed animals have up to 100% of EB-stained nuclei. The < 5% of hepatopancreatic tubes nuclei stained with EB were classified as 0, and those with the highest proportion (> 95%) of EB stained nuclei as 9.²¹

Micro-PIXE analysis: Tissue distribution of Co and Fe

For microparticle induced x-ray emission (micro-PIXE) analysis, digestive glands were shock-frozen in liquid propane or N₂, using tissue-freezing medium (Jung Tissue Freezing Medium, Leica). Samples were sectioned with a section thickness of 60 μm using a Leica CM3050 cryotome (Leica) with the temperature of the microtome head and chamber

1
2
3 maintained between -25°C and -20°C . The sections were placed in pre-cooled Al holders,
4 transferred to an alpha 2-4 Christ freeze dryer using a cryo-transfer assembly cooled with
5 liquid N_2 , and then freeze-dried at -30°C and 0.4 mbar for 24 h. Dry sections were mounted
6 between two thin layers of Pioloform foil on the Al sample holder.^{26, 27}
7
8

9
10 For detection of X-rays between 1 keV and 25 keV, two X-ray detectors were used
11 simultaneously. A high-purity germanium X-ray detector (active area 95 mm^2 ; beryllium
12 window, $25\text{ }\mu\text{m}$ thick; polyimide absorber, $100\text{ }\mu\text{m}$ thick) positioned at 135° to the beam
13 direction was used for the energy range of 4 keV–25 keV. Low energy X-rays in the range of
14 0.8 keV – 6 keV were detected by a Si(Li) detector (active area 10 mm^2) positioned at 125° to
15 the beam direction. The proton dose was determined by a rotating in-beam chopper.
16 Measurement of micro-PIXE emission and data evaluation for the biological samples of
17 intermediate thickness at the micro-PIXE laboratory, previously described in detail,^{26, 28, 29}
18 was performed at the Jožef Stefan Institute in Ljubljana.
19
20
21
22
23
24

25
26 We analysed cross sections of isolated digestive glands tubes from six animals. Two
27 analysed animals were control ones, two were fed on food dosed with $2000\text{ }\mu\text{g/g}$ with CoCl_2
28 and two animals on food dosed with $2000\text{ }\mu\text{g/g}$ nano- CoFe_2O_4 . Three or two digestive gland
29 tubes were isolated from each animal and analysed.
30
31
32

33 34 35 **LE-XRF analysis: Cell distribution and co-localization of Co and Fe in digestive gland** 36 **cells** 37

38
39 For Low Energy Synchrotron Radiation X-ray Fluorescence (LE-XRF) analysis,
40 isolated digestive glands were shock-frozen in liquid N_2 , using tissue-freezing medium (Jung
41 Tissue Freezing Medium, Leica). Samples were sectioned with a section thickness of $14\text{ }\mu\text{m}$
42 using a Leica CM3050 cryotome (Leica) with the temperature of the microtome head and
43 chamber maintained between -25°C and -20°C . The sections were placed in pre-cooled Al
44 holders, transferred to an alpha 2-4 Christ freeze dryer using a cryo-transfer assembly cooled
45 with liquid N_2 , and then freeze-dried at -30°C and 0.4 mbar for 24 h. Dry sections were
46 mounted between two thin layers of Pioloform foil on the sample holder.
47
48
49
50
51
52

53
54 LE-XFR experiments were carried out at the Elettra synchrotron radiation facility in
55 Trieste with the TwinMic beamline, a soft X-ray transmission microscope^{30, 31} operating in the
56 400 – 2200 eV photon energy range. During the experiments TwinMic was operated in STXM
57
58
59
60

1
2
3 mode,³¹ in which a microprobe is formed by a zone plate lens and the specimen is raster
4 scanned across it. The TwinMic microscope can provide sub-micron spatial resolution, but we
5 used a spot size and a step size of 1 μ m, which is a useful compromise between lateral
6 resolution adequate for the features of interest and good XRF signal.
7
8

9
10 The STXM mode allows simultaneous acquisition of X-ray transmission (absorption
11 and phase contrast images) and photon emission (XRF) signals.³² The low X-ray energy range
12 is particularly suited to biological investigations, and allows the simultaneous acquisition of
13 the elemental distributions of elements of low atomic number (B to P) from the K emission
14 lines and elements of higher atomic number (Ca to Nb) from the L emission lines. The
15 absorption and phase contrast images are collected by a configurable detector arrangement
16 consisting of a fast read-out electron multiplying CCD camera coupled to an X-ray-to-visible
17 light conversion system. The LEXRF set-up used for this experiment consists of an annular
18 arrangement of 8 Si drift detectors (SDDs) (PNSensor, Munich, Germany), only 5 of which,
19 coupled to read-out electronics, were used.^{33, 34} This arrangement currently allows only
20 qualitative analyses. Full elemental quantification will be the subject of future reports.
21
22
23
24
25
26
27
28

29
30 The X-ray fluorescence spectra obtained for each pixel in the raster scan were batch
31 processed by fitting the peaks with a Gaussian model and with a linear subtraction, using the
32 PyMCA data analysis software.³⁵ Elemental maps were generated by plotting the intensity of
33 the fluorescence peaks as a function of their position in the sample plane.
34
35
36

37 In experiment A (see Table S1, Supporting Information), a cross section of one
38 isolated gland from control animal, two isolated glands from one animal fed on food dosed
39 with 2000 μ g/g CoCl₂ and two sections of digestive gland tubes from one animal fed on food
40 dosed with 2000 μ g/g CoFe₂O₄ nanoparticles were analysed. In experiment B samples from
41 one control animal and two sections from two animals from each treated group (animals fed
42 on food dosed with 2000 μ g/g CoCl₂ or CoFe₂O₄ nanoparticles) were analysed. In experiment
43 C two sections from two different animals both fed on food dosed with 2000 μ g/g nano-
44 CoFe₂O₄ were analysed. All together 12 different cross sections of digestive glands were
45 analysed.
46
47
48
49
50
51

52 **AAS Analysis: Concentration of Co and Fe in digestive glands**

53
54
55 Cobalt and iron were measured by atomic absorption spectroscopy in one or two
56 isolated digestive gland tubes from each animal in experiment A and D. Prior to the analysis,
57
58
59
60

1
2
3 samples were lyophilized, weighed, and completely digested in a 7:1 nitric acid/perchloric
4 acid mixture. After evaporation of the acid, the residue was taken up in 0.2 % HNO₃ and total
5 Co and Fe concentrations in the digestive glands were determined by flame atomic absorption
6 spectrometry (Perkin Elmer AAnalyst 100) in the Department of Biology, University of
7 Ljubljana. Reagent blanks and standard solutions (Merck) were used to ensure accuracy and
8 precision in the analysis.
9
10
11
12

13 **Concentration of Co in the supernatant of the nano-CoFe₂O₄ suspensions**

14
15 For the analysis, 1000 mg/L and 2000 mg/L suspensions of CoFe₂O₄ NPs in bidistilled
16 water were prepared in the same way as for the *in vivo* tests. The suspensions were
17 ultracentrifuged at 100,000 g for 30 min at 20°C. The pellet formed by nanoparticles was
18 separated from the supernatant which was again ultracentrifuged at 100,000 g for 30 min at
19 20°C. Then the supernatant was separated from the pellet and divided into two aliquots for
20 further dilution. One aliquot was diluted with an equal volume of bidistilled water, the other
21 with an equal volume of 1M HCl. Then 2 ml from each aliquot was analyzed by flame atomic
22 absorption spectrometry (Perkin Elmer Analyst 100) in the Department of Biology. The
23 difference in cobalt ion content between the acidified and non-acidified suspension indicates
24 that nanoparticles remaining in the supernatant after centrifugation are dissolved. Detection of
25 cobalt by AAS would be possible provided that the concentration of ionized Co is above the
26 detection limit (9 µg/L).
27
28
29
30
31
32
33
34

35 The original suspensions of CoFe₂O₄ NPs (1000 and 2000 mg/L of CoFe₂O₄) were
36 also analysed by AAS. Prior to the analysis the suspensions were diluted (1:1000) with
37 distilled water and HCl to see if dilution medium effects the measurements by dissolving the
38 nanoparticles in the solutions.
39
40
41
42

43 **Data analysis**

44
45
46 Data were analysed by standard statistical methods. The difference in the median
47 measured parameters in exposed and unexposed groups was tested with the non-parametric
48 Mann-Whitney U test. All calculations were performed with Statgraphics Plus 4.0.
49 Statistically significant differences between exposed and control animals were divided into
50 three categories with different numbers of stars assigned (* $p < 0.05$, ** $p < 0.01$, *** $p <$
51 0.001).
52
53
54
55
56
57
58
59
60

Results

Characterization of nanoparticles

TEM analysis showed the nanoparticles to have a relatively broad size distribution between 5 and 15 nm (Figure S1A, Supporting Information). The smaller nanoparticles are globularly shaped; while the larger ones have an octahedral shape. Energy dispersive X-ray spectroscopy (EDS) analysis showed that their composition matched to stoichiometry of CoFe_2O_4 .

Zeta potential measurements showed the isoelectric point for CoFe_2O_4 nanoparticles at neutral pH. At pH 7.4 zeta potential is slightly negative. SEM revealed that particles remained spread over the entire leaf surface (Figure S1B, Table S2, Supporting Information) and energy dispersive X-ray analysis (EDX) revealed their chemical composition (Table S2, Supporting Information).

Feeding parameters, weight change and mortality

Animals were exposed to leaves dosed with CoCl_2 or a suspension of CoFe_2O_4 NPs, providing nominal concentrations of 1000, 2000 or 5000 μg CoCl_2 or CoFe_2O_4 nanoparticles per g of leaf. Weight and survival were not affected at this level of additive. In all four experiments there was a statistically significant difference in feeding rate between control groups and groups in which animals were exposed to 2000 or 5000 $\mu\text{g}/\text{g}$ of CoCl_2 . Exposure to CoFe_2O_4 nanoparticles had no effect on the feeding rate of animals in any experiment for the 14 days of the experiment. Compared to the control animals, the reduction in the feeding rate of animals exposed to CoCl_2 was statistically significant in higher concentrations (2000, 5000 $\mu\text{g}/\text{g}$) of Co in food as shown in Figure S2 (Supporting Information).

AO/EB analysis: Digestive gland cell membrane stability

Our previously published data demonstrate that the digestive gland cell membrane stability value was higher than 2 (on a scale from 0 to 9) in only 5% of animals from a stock culture and in good physiological condition, and this number was used as a benchmark.²¹ The cell membranes are considered destabilised when this value is higher than 2.

1
2
3 We combine results on cell membrane stability from all three experiments (A, B and
4 C). The cell membrane stability of controls was not affected in more than ~10% of the
5 animals and this was considered to be normal. An exposure concentration of 1000 $\mu\text{g CoCl}_2/\text{g}$
6 in the food caused digestive gland cell membrane destabilization in up to 40% of exposed
7 animals and an exposure concentration of 2000 $\mu\text{g CoCl}_2/\text{g}$ in the food caused destabilization
8 in up to 30% of exposed animals. Upon exposure to 1000 or 2000 $\mu\text{g nano-CoFe}_2\text{O}_4$ per g dry
9 weight of leaves, approximately 10% and 20% of exposed animals respectively had
10 destabilized digestive cell membrane. This is not statistically significantly different from
11 controls, where one animal out of 22, had destabilized cell membrane. In animals exposed to
12 Co, four animals out of a group of 10 animals fed with 1000 $\mu\text{g CoCl}_2/\text{g}$ dry weight of leaf
13 and three from a group fed with 1000 $\mu\text{g CoCl}_2/\text{g}$ dry weight of leaf had destabilized cell
14 membrane. The highest proportion of animals with destabilised membranes was found in a
15 group fed on food containing 1000 $\mu\text{g CoCl}_2/\text{g}$ dry weight of leaf, but this was not
16 significantly different from a group of animals fed with 2000 $\mu\text{g CoCl}_2/\text{g}$ dry weight of leaf
17 (Figure 1).
18
19
20
21
22
23
24
25
26
27
28
29
30

31 **Micro-PIXE analysis: Tissue distribution of Co and Fe**

32
33 In the micro-PIXE analysis, the concentrations of elements with values above
34 Minimum Limits Of Detection (MLDs) are simultaneously analyzed. In parallel to the
35 distribution of Co and Fe in the tissue, the distribution of Cu is determined, indicating the
36 locations of metal storing granules in S-cells of digestive gland epithelium.
37
38
39

40 In all the samples analysed, the concentrations of Fe were similar. In all the animals
41 exposed to food dosed with CoFe_2O_4 NPs, concentrations of Co were statistically significantly
42 higher than those measured in controls, where in most cases Co was below limit of detection
43 (Figure 2A). As expected, very high concentrations of Co were also detected in animals fed
44 with CoCl_2 -dosed food (Figure 2B). Overlap with Cu was observed (Figure 2, Panels B and
45 C) in all cases where Co was found in the epithelium. This co-localisation indicates that Co
46 either originating from CoCl_2 or from nano- CoFe_2O_4 is stored in metal storing granules of S-
47 cells. LE-XRF was used to assess co-localisation of Co and Fe in gland epithelium. This
48 provides better spatial resolution (1 μm) allowing analysis at subcellular length scales. The
49 same XRF protocol has been used successfully to analyse cellular distribution and
50 degradation of CoFe_2O_4 NPs in fibroblast cells.²²
51
52
53
54
55
56
57
58
59
60

LE-XRF analysis: Cell distribution and colocalization of Co and Fe in digestive gland cells

To confirm the data obtained with PIXE and gather information at the subcellular level, LE-XRF analyses were used to study co-localisation of Co and Cu which was observed in all the samples. Outside this region Co was not detected. These results confirmed the absence of co-localization of Co and Fe but Fe was found at some other locations (Figure 3A and 3B), indicating either the presence of Fe in the animals before the experiment or production of Fe from the particles. Since the concentrations of Fe analysed by other methods (PIXE, AAS) did not show any increase of Fe in animals exposed to CoFe_2O_4 nanoparticles, we concluded that Fe is not derived in substantial amounts from CoFe_2O_4 nanoparticles.

AAS Analysis: Concentration of Co and Fe in digestive glands

After 14 days exposure of animals to CoCl_2 and CoFe_2O_4 NPs, the amounts of Co (experiments A and D) and Fe (experiment D) in digestive glands were measured. The amount of Co showed a statistically significant increase in both experiments in which animals were exposed to CoCl_2 . This indicates that more Co accumulated when animals were exposed to Co ions as compared to nanoparticles. Statistically significant changes in experiment D occur among control animals and all exposed animals (Figure 4A). These results show that accumulation of Co in hepatopancreas is dose-dependent. No Fe accumulation was detected when animals were fed CoFe_2O_4 nanoparticles (Figure 4B).

Chemical analysis of Co dissolution from CoFe_2O_4 nanoparticles

All measurements of the supernatants fell below the detection limit of AAS analysis and we were able to conclude that levels of cobalt in the supernatant were below $0.009 \mu\text{g/ml}$.

With AAs, the CoFe_2O_4 NPs suspension gave reliable measurements. The suspension with the concentration of $1000 \mu\text{g/L}$ of cobalt gave values of approximately $600\text{-}700 \mu\text{g/L}$ when diluted with distilled water and approximately $800 \mu\text{g/L}$ when diluted with HCl. The second suspension, with a concentration of $2000 \mu\text{g/L}$ of cobalt also gave higher measured values when diluted with HCl compared with distilled water. The values were approximately $1200 \mu\text{g/L}$ for distilled water and $1800 \mu\text{g/L}$ for HCl. The above values indicate that cobalt NPs dissolved in an acid solution, allowing better detection of cobalt by AAS.

Discussion

Feeding of the model terrestrial invertebrate *P. scaber* on food dosed with CoFe_2O_4 nanoparticles or Co ions (1000, 2000, or 5000 $\mu\text{g/g}$ of leaf of CoCl_2 or nano- CoFe_2O_4) resulted in intracellular accumulation of Co ions, but not of particles. Toxic effects were ascribed to Co ions rather than CoFe_2O_4 nanoparticles themselves.

We have shown in our *in vivo* study that the observed toxicity as evidenced by reduced feeding rate and cytotoxicity as manifested by cell membrane stability are correlated to available metal ions in the food. The effect on feeding rate was dose dependent while cell membrane destabilisation was not significantly different between animals exposed to 1000 or 2000 $\mu\text{g/g}$ of CoCl_2 . This leads to the conclusion that if amount of Co available in the food is high enough, it leads to cytotoxic effects. Available metal ions were inferred from the amount of accumulated Co^{2+} in the digestive gland cells and this amount was higher when animals were fed with food dosed with CoCl_2 than when with CoFe_2O_4 nanoparticles.

We have shown by x-ray-based techniques that only Co, but not Fe entered cells. Cobalt was always found to be co-localized with Cu and this indicates that Co follows the same cellular pathways as other metal ions, such as Cu^{2+} which are transported to metal storage granules where they accumulate. This suggests that only ions generated from CoFe_2O_4 nanoparticles or available from CoCl_2 salt are internalised and that Co^{2+} accumulation is dose-dependent.

Other authors report that Co nanoparticles and Co ions are both responsible for the effects on cells and explain that the nature of the effects depends on the type of the cell line, duration of exposure and applied nanoparticle concentration.¹⁵ Ponti et al.²³ reported that toxicity was higher for Co nanoparticles than for Co ions after 2 and 24 hours exposure, while Papis et al.¹⁴ showed that CoCl_2 has a more severe cytotoxic effect on human cell lines compared to Co_3O_4 nanoparticles.

Dissolution of Co ions from nanoparticles has also been reported. Papis et al.¹⁴ evaluated spontaneous dissolution of Co ions from Co_3O_4 NPs in Phosphate buffered saline (PBS), distilled H_2O and culture medium. Their results showed that release of Co^{2+} from NPs takes place in every tested medium but remains under 1% of the total Co in media. The percentage of leaching of Co ions from Co NPs in Dulbecco's Modified Eagle Medium

(DMEM) was determined by Horev-Azaria et al.¹⁵ who found that incubation of the Co NPs for the 72 h resulted in decomposition of $44 \pm 10\%$ of the Co-NPs.

In our study we also used ultracentrifugation to measure the release of Co from CoFe nanoparticles in distilled water. The level of Co in supernatants was found to be below the detection limit of AAS instrument ($0.009 \mu\text{g/ml}$). The animals assimilated an average of approximately 7% of consumed cobalt when fed with Co salts, and between 1% and 2% of cobalt when fed with cobalt nanoparticles. These data are not in agreement with the extremely low levels ($< 0.009 \mu\text{g/ml}$) of dissolved Co indicated by the ultracentrifugation experiments. This finding suggests that the majority of assimilated Co decomposes inside the digestive system of tested animals and not in the suspension which was applied to the leaves. This is in agreement with our other studies on ZnO and CuCe (unpublished data).

The potential dissolution of particles inside organisms has not been intensively studied before. More attention was given to chemical analytical methods for measuring dissolution of particles from suspensions in different suspensions. We propose the use of a model biological system with a terrestrial isopod for studying potential dissolution of ions from metal containing nanoparticles in biologically complex media. A system which allows measuring dissolution of a variety of nanoparticles with different modifications is important to properly characterise particles before biomedical application as well as in the food industry.

Author information

Corresponding author

Phone: + 386 1 423 33. Fax: +386 1 257 33 90. E-mail: damjana.drobne@bf.uni-lj.si

Notes

The authors declare no competing financial interest

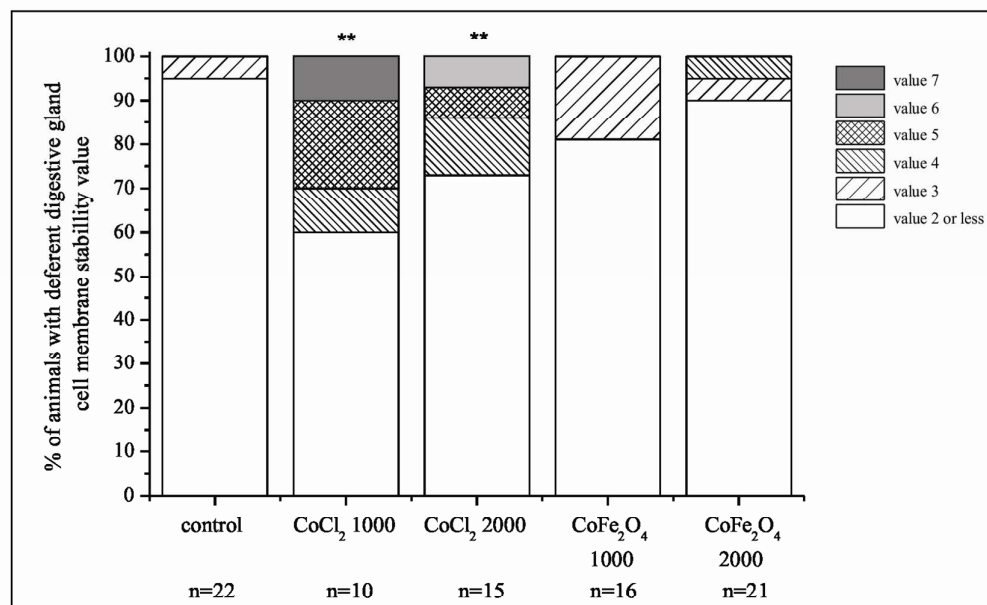


Figure 1. Percentage of animals in each exposure group in experiments A, B, and C with different degrees of destabilised cell membrane. Destabilization of the cell membrane was assessed visually and classified from 0 to 9 according to the predefined scale described in Materials and Methods. Digestive gland cell membrane stability value of 2 or less denotes animals which did not have destabilized cell membranes and digestive gland cell membrane stability values from 3 to 9 animals with some degree of destabilization of the cell membranes. A value of 7 corresponds to the most highly destabilized cell membranes. Statistical significant differences between exposed and control animals are marked with ** ($p < 0.01$). Nominal exposure concentrations (1000 or 2000 $\mu\text{g CoCl}_2$ or nano- $\text{CoFe}_2\text{O}_4/\text{g}$ of leaf) and number of animals per group (n) are provided on the x-axis.

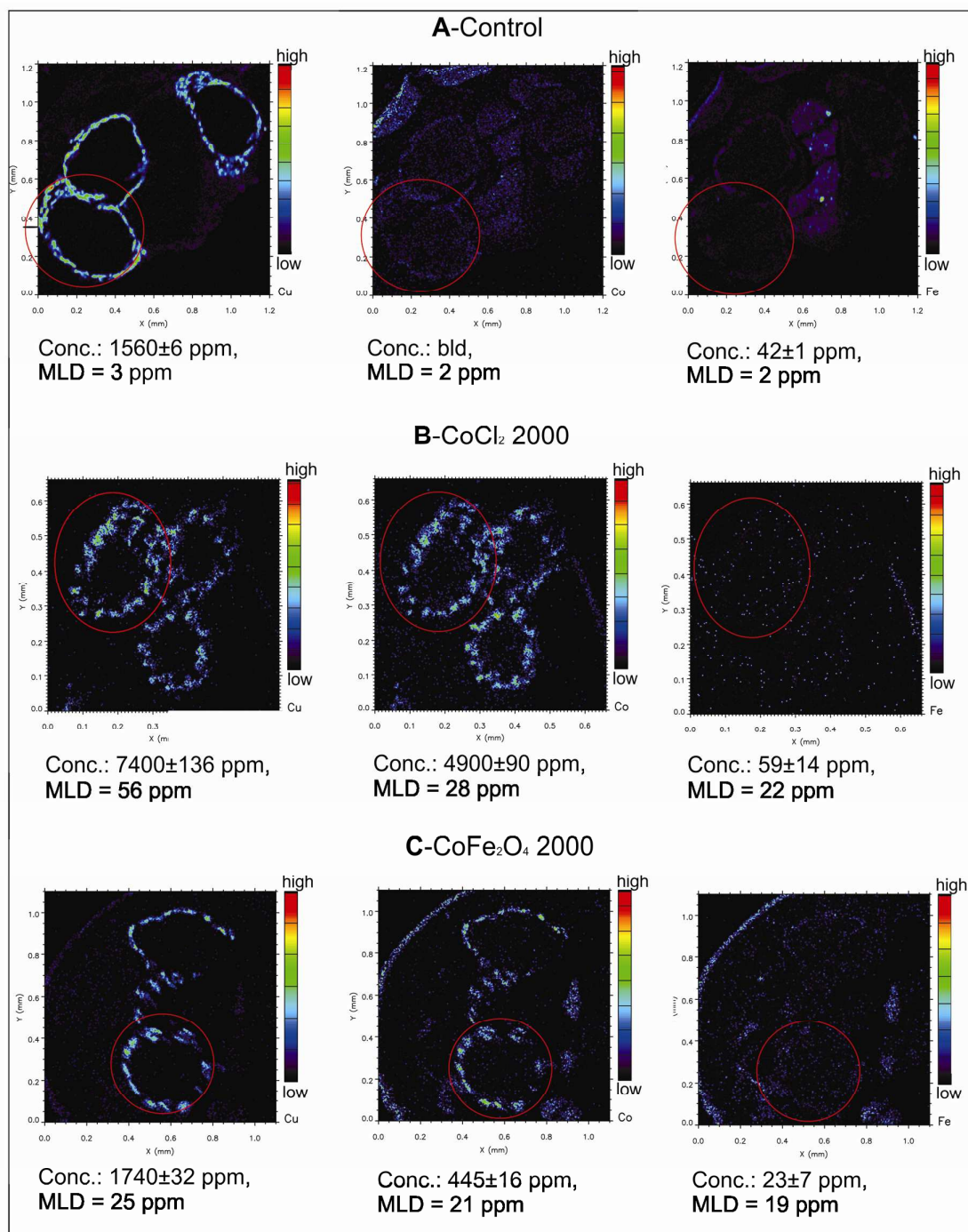


Figure 2. PIXE analyses of digestive gland cross section and corresponding concentrations of measured elements. (A) Elemental maps of Cu, Co and Fe in digestive glands of a control animal. (B) Cross section of digestive glands of animal exposed to food dosed with $2000 \mu\text{g CoCl}_2/\text{g}$ dry weight of food. (C) cross section of digestive glands of animal exposed to food dosed with $2000 \mu\text{g nano-CoFe}_2\text{O}_4/\text{g}$ dry weight of food. The elemental maps present the cross sections of three digestive gland tubes. Under each map, the

concentrations of elements for selected encirculated glands are provided together with corresponding Minimum Limit of Detection (MLD).

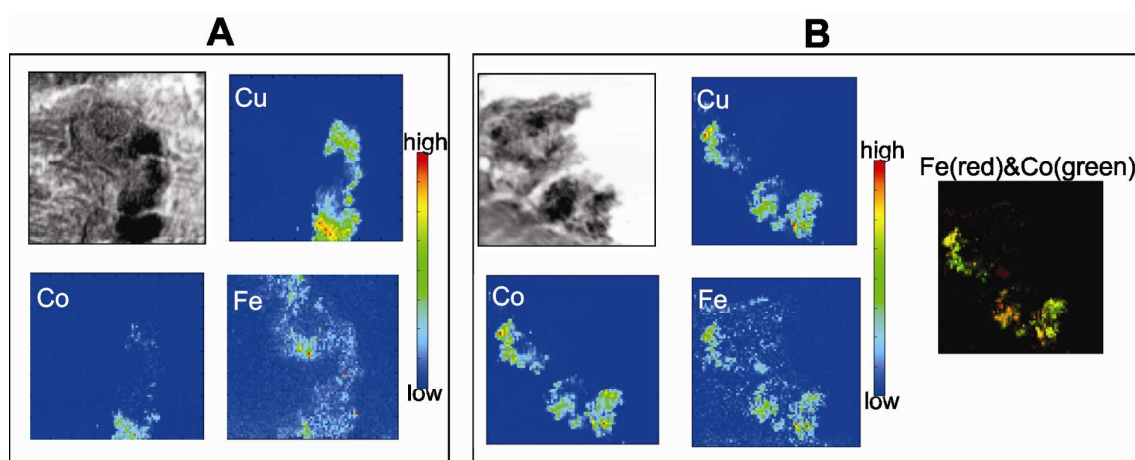


Figure 3. $80 \times 80 \mu\text{m}^2$ x-ray absorption images of part of digestive gland epithelium and the corresponding XRF maps. The distribution of Cu, Fe and Co in control animal (A) and in animal fed with food dosed with $2000 \mu\text{g}$ nano- CoFe_2O_4 / g dry weight of food (B). The co-localization of Co and Cu and Co and Fe for the fed animal are shown in (B) as well. All images and XRF maps were collected using photon energy of 1.14 keV.

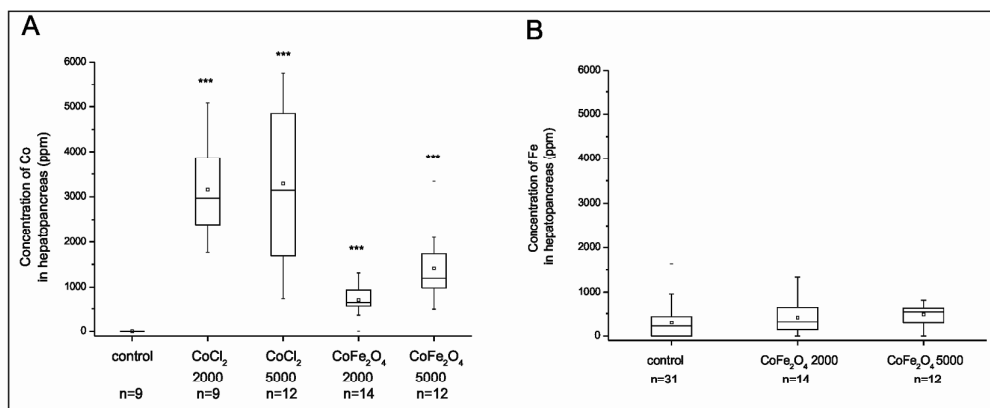


Figure 4. Concentration of Co or Fe in hepatopancreas after 14 days of feeding with CoCl₂ salts or nano-CoFe₂O₄ dosed food in experiment D, measured by AAS. (A) concentration of Co in hepatopancreas in experiment D. (B) Concentration of Fe in hepatopancreas in experiment D. Symbols on the box plot represent minimum and maximum data values (whiskers), mean value (□), 75th percentile (upper edge of box), 25th percentile (lower edge of box), median (line in box) and max and min value (-). Statistical differences between exposed and control animals are marked with * ($p < 0.001$). Nominal exposure concentration (2000 or 5000 μg CoCl₂ or nano-CoFe₂O₄/g of leaf) and number of animals per group (n) are provided on x-axis. Ppm stands for unit $\mu\text{g/g}$.**

Acknowledgements

Work of PhD student Sara Novak was supported by Slovenian Research Agency within the framework of young researchers. Part of work was conducted within research projects financed by Slovenian Research Agency (J1-4109) and within the 7th FP EU Project “NANOVALID” (contract: 263147). We thank G.W.A Milne for editorial assistance and Matej Hočevar from Institute of metals and technology Institute, Ljubljana for scanning electron micrographs.

References

(1) Zi, Z. F.; Sun, Y. P.; Zhu, X. B.; Yang, Z. R.; Dai, J. M.; Song, W. H., Synthesis and magnetic properties of CoFe₂O₄ ferrite nanoparticles. *J Magn Magn Mater* **2009**, *321*, (9), 1251-1255.

(2) Baldi, G.; Bonacchi, D.; Innocenti, C.; Lorenzi, G.; Sangregorio, C., Cobalt ferrite nanoparticles: The control of the particle size and surface state and their effects on magnetic properties. *Journal of Magnetism and Magnetic Materials* **2007**, *311*, (1), 10-16.

(3) Mornet, S.; Vasseur, S.; Grasset, F.; Veverka, P.; Goglio, G.; Demourgues, A.; Portier, J.; Pollert, E.; Duguet, E., Magnetic nanoparticle design for medical applications. *Progress in Solid State Chemistry* **2006**, *34*, (2-4), 237-247.

(4) Joshi, H. M.; Lin, Y. P.; Aslam, M.; Prasad, P. V.; Schultz-Sikma, E. A.; Edelman, R.; Meade, T.; Dravid, V. P., Effects of Shape and Size of Cobalt Ferrite Nanostructures on Their MRI Contrast and Thermal Activation. *Journal of Physical Chemistry C* **2009**, *113*, (41), 17761-17767.

(5) Arruebo, M.; Fernandez-Pacheco, R.; Ibarra, M. R.; Santamaria, J., Magnetic nanoparticles for drug delivery. *Nano Today* **2007**, *2*, (3), 22-32.

(6) Chemla, Y. R.; Crossman, H. L.; Poon, Y.; McDermott, R.; Stevens, R.; Alper, M. D.; Clarke, J., Ultrasensitive magnetic biosensor for homogeneous immunoassay. *Proceedings of the National Academy of Sciences of the United States of America* **2000**, *97*, (26), 14268-14272.

(7) Hergt, R.; Dutz, S.; Muller, R.; Zeisberger, M., Magnetic particle hyperthermia: nanoparticle magnetism and materials development for cancer therapy. *Journal of Physics-Condensed Matter* **2006**, *18*, (38), S2919-S2934.

(8) Salloum, M.; Ma, R. H.; Weeks, D.; Zhu, L., Controlling nanoparticle delivery in magnetic nanoparticle hyperthermia for cancer treatment: Experimental study in agarose gel. *International Journal of Hyperthermia* **2008**, *24*, (4), 337-345.

(9) Zou, W. G.; Yan, M. D.; Xu, W. J.; Huo, H. R.; Sun, L. Y.; Zheng, Z. C.; Liu, X. Y., Cobalt chloride induces PC12 cells apoptosis through reactive oxygen species and accompanied by AP-1 activation. *Journal of Neuroscience Research* **2001**, *64*, (6), 646-653.

(10) Petit, A.; Mwale, F.; Tkaczyk, C.; Antoniou, J.; Zukor, D. J.; Huk, O. L., Induction of protein oxidation by cobalt and chromium ions in human U937 macrophages. *Biomaterials* **2005**, *26*, (21), 4416-4422.

1
2
3 (11) De Boeck, M.; Lison, D.; Kirsch-Volders, M., Evaluation of the in vitro direct and
4 indirect genotoxic effects of cobalt compounds using the alkaline comet assay. Influence of
5 interdonor and interexperimental variability. *Carcinogenesis* **1998**, *19*, (11), 2021-2029.

6
7
8 (12) Dokoumetzidis, A.; Macheras, P., A century of dissolution research: From Noyes and
9 Whitney to the Biopharmaceutics Classification System. *Int J Pharm* **2006**, *321*, (1-2), 1-11.

10
11 (13) Miao, A. J.; Zhang, X. Y.; Luo, Z. P.; Chen, C. S.; Chin, W. C.; Santschi, P. H.;
12 Quigg, A., Zinc Oxide Engineered Nanoparticles Dissolution and Toxicity to Marine
13 Phytoplankton. *Environmental Toxicology and Chemistry* **2010**, *29*, (12), 2814-2822.

14
15 (14) Papis, E.; Rossi, F.; Raspanti, M.; Dalle-Donne, I.; Colombo, G.; Milzani, A.;
16 Bernardini, G.; Gornati, R., Engineered cobalt oxide nanoparticles readily enter cells. *Toxicol*
17 *Lett* **2009**, *189*, (3), 253-259.

18
19 (15) Horev-Azaria, L.; Kirkpatrick, C. J.; Korenstein, R.; Marche, P. N.; Maimon, O.;
20 Ponti, J.; Romano, R.; Rossi, F.; Golla-Schindler, U.; Sommer, D.; Ubaldi, C.; Unger, R. E.;
21 Villiers, C., Predictive Toxicology of Cobalt Nanoparticles and Ions: Comparative In Vitro
22 Study of Different Cellular Models Using Methods of Knowledge Discovery from Data.
23 *Toxicological Sciences* **2011**, *122*, (2), 489-501.

24
25 (16) Zook, J. M.; Long, S. E.; Cleveland, D.; Geronimo, C. L. A.; MacCuspie, R. I.,
26 Measuring silver nanoparticle dissolution in complex biological and environmental matrices
27 using UV-visible absorbance. *Analytical and Bioanalytical Chemistry* **2011**, *401*, (6), 1993-
28 2002.

29
30 (17) Zimmer, M.; Topp, W., Homeostatic responses in the gut of Porcellio scaber (Isopoda:
31 Oniscidea) optimize litter degradation. *Journal of Comparative Physiology B-Biochemical*
32 *Systemic and Environmental Physiology* **1997**, *167*, (8), 582-585.

33
34 (18) Zimmer, M.; Brune, A., Physiological properties of the gut lumen of terrestrial
35 isopods (Isopoda : Oniscidea): adaptive to digesting lignocellulose? *Journal of Comparative*
36 *Physiology B-Biochemical Systemic and Environmental Physiology* **2005**, *175*, (4), 275-283.

37
38 (19) Udovic, M.; Drobne, D.; Lestan, D., Bioaccumulation in Porcellio scaber (Crustacea,
39 Isopoda) as a measure of the EDTA remediation efficiency of metal-polluted soil.
40 *Environmental Pollution* **2009**, *157*, (10), 2822-2829.

41
42 (20) Pipan-Tkalec, Z.; Drobne, D.; Jemec, A.; Romih, T.; Zidar, P.; Bele, M., Zinc
43 bioaccumulation in a terrestrial invertebrate fed a diet treated with particulate ZnO or ZnCl₂
44 solution. *Toxicology* **2010**, *269*, (2-3), 198-203.

1
2
3 (21) Valant, J.; Drobne, D.; Sepcic, K.; Jemec, A.; Kogej, K.; Kostanjsek, R., Hazardous
4 potential of manufactured nanoparticles identified by in vivo assay. *Journal of Hazardous*
5 *Materials* **2009**, *171*, (1-3), 160-165.

6
7
8 (22) Marmorato, P.; Ceccone, G.; Gianoncelli, A.; Pascolo, L.; Ponti, J.; Rossi, F.; Salome,
9 M.; Kaulich, B.; Kiskinova, M., Cellular distribution and degradation of cobalt ferrite
10 nanoparticles in Balb/3T3 mouse fibroblasts. *Toxicol Lett* **2011**, *207*, (2), 128-136.

11
12 (23) Ponti, J.; Sabbioni, E.; Munaro, B.; Broggi, F.; Marmorato, P.; Franchini, F.;
13 Colognato, R.; Rossi, F., Genotoxicity and morphological transformation induced by cobalt
14 nanoparticles and cobalt chloride: an in vitro study in Balb/3T3 mouse fibroblasts.
15 *Mutagenesis* **2009**, *24*, (5), 439-445.

16
17 (24) Gyergyek, S.; Drofenik, M.; Makovec, D., Oleic-acid-coated CoFe₂O₄ nanoparticles
18 synthesized by co-precipitation and hydrothermal synthesis. *Mater Chem Phys* **2012**, *133*, (1),
19 515-522.

20
21 (25) Mcgahon, A. J.; Martin, S. J.; Bissonnette, R. P.; Mahboubi, A.; Shi, Y. F.; Mogil, R.
22 J.; Nishioka, W. K.; Green, D. R., The End of the (Cell) Line - Methods for the Study of
23 Apoptosis in-Vitro. *Methods in Cell Biology, Vol 46* **1995**, *46*, 153-185.

24
25 (26) Vogel-Mikus, K.; Pelicon, P.; Vavpetic, P.; Krett, I.; Regvar, M., Elemental analysis
26 of edible grains by micro-PIXE: Common buckwheat case study. *Nuclear Instruments &*
27 *Methods in Physics Research Section B-Beam Interactions with Materials and Atoms* **2009**,
28 *267*, (17), 2884-2889.

29
30 (27) Schneider, T.; Strasser, O.; Gierth, M.; Scheloske, S.; Povh, B., Micro-PIXE
31 investigations of apoplatic iron in freeze-dried root cross-sections of soil grown barley.
32 *Nuclear Instruments & Methods in Physics Research Section B-Beam Interactions with*
33 *Materials and Atoms* **2002**, *189*, 487-493.

34
35 (28) Vogel-Mikus, K.; Pongrac, P.; Kump, P.; Necemer, M.; Simcic, J.; Pelicon, P.;
36 Budnar, M.; Povh, B.; Regvar, M., Localisation and quantification of elements within seeds of
37 Cd/Zn hyperaccumulator *Thlaspi praecox* by micro-PIXE. *Environmental Pollution* **2007**,
38 *147*, (1), 50-59.

39
40 (29) Vogel-Mikus, K.; Regvar, M.; Mesjasz-Przybylowicz, J.; Przybylowicz, W. J.;
41 Simcic, J.; Pelicon, P.; Budnar, M., Spatial distribution of cadmium in leaves of metal
42 hyperaccumulating *Thlaspi praecox* using micro-PIXE. *New Phytologist* **2008**, *179*, (3), 712-
43 721.

1
2
3 (30) Kaulich B, S. J., David C, Di Fabrizio E, Morrison G, Charalambous P et al, A
4 European Twin X-ray Microscopy Station Commissioned at ELETTRA. *In Proceeding of 8th*
5 *International Conference on X-ray micros, Conf Proc Series IPAP 2006*, 7, 22-25.

6
7
8 (31) Kaulich, B.; Thibault, P.; Gianoncelli, A.; Kiskinova, M., Transmission and emission
9 x-ray microscopy: operation modes, contrast mechanisms and applications. *Journal of*
10 *Physics-Condensed Matter 2011*, 23, (8).

11
12 (32) Morrison, G. R.; , A. G.; , B. K.; , D. B.; Kovac, a. J., A Fast-readout CCD System for
13 Configured-Detector Imaging in STXM. *Proc. 8th Int. Conf. X-ray Microscopy IPAP Conf.*
14 *Series 2006*, 7, 377-379.

15
16 (33) Alberti, R.; Klatka, T.; Longoni, A.; Bacescu, D.; Marcello, A.; De Marco, A.;
17 Gianoncelli, A.; Kaulich, B., Development of a low-energy x-ray fluorescence system with
18 sub-micrometer spatial resolution. *X-Ray Spectrometry 2009*, 38, (3), 205-209.

19
20 (34) Gianoncelli, A.; Kaulich, B.; Alberti, R.; Klatka, T.; Longoni, A.; de Marco, A.;
21 Marcello, A.; Kiskinova, M., Simultaneous soft X-ray transmission and emission microscopy.
22 *Nuclear Instruments & Methods in Physics Research Section a-Accelerators Spectrometers*
23 *Detectors and Associated Equipment 2009*, 608, (1), 195-198.

24
25 (35) Sole, V. A.; Papillon, E.; Cotte, M.; Walter, P.; Susini, J., A multiplatform code for
26 the analysis of energy-dispersive X-ray fluorescence spectra. *Spectrochimica Acta Part B-*
27 *Atomic Spectroscopy 2007*, 62, (1), 63-68.
28
29
30
31
32
33
34
35
36
37
38
39
40
41
42
43
44
45
46
47
48
49
50
51
52
53
54
55
56
57
58
59
60